

WAVE-PARTICLE INTERACTIONS AT THE MAGNETOPAUSE: CONTRIBUTIONS TO THE DAYSIDE AURORA

B. T. Tsurutani<sup>1</sup>, E. J. Smith<sup>1</sup>, R. M. Thorne<sup>2</sup>, R. R. Anderson<sup>3</sup>, D. A. Gurnett<sup>3</sup>, G. K. Parks<sup>4</sup>, C. S. Lin<sup>5</sup>, and C. T. Russell<sup>2</sup>

<sup>1</sup>Jet Propulsion Laboratory, California Institute of Technology, Pasadena, California 91109

<sup>2</sup>University of California at Los Angeles, Los Angeles, California 90024

<sup>3</sup>University of Iowa, Iowa City, Iowa 52242

<sup>4</sup>University of Washington, Seattle, Washington 98105

<sup>5</sup>University of Maryland, College Park, Maryland 20742

Abstract

A strong correlation between intense, broad-band 10-10<sup>5</sup> Hz plasma waves and 1-6 keV electrons and protons are observed on ISEE 1 and 2 at the low latitude dayside magnetopause. Wave and particle features have been characterized by taking averages over ten events. The 10-10<sup>3</sup> Hz magnetic waves and the 10-10<sup>5</sup> Hz electric emissions can be represented by the power-law spectra,  $I_m = 10 f^{-3.9} \text{ nT}^2/\text{Hz}$  and  $I_e = 3 \times 10^{-5} f^{2.8} \text{ V}^2/\text{m}^2 \text{ Hz}$ , respectively. The electron and proton fluxes and spectral shapes are nearly constant from event-to-event, and are characterized by  $j^- = 3 \times 10^5 \text{ E}^{-1.8} \text{ cm}^{-2} \text{ sec}^{-1} \text{ ster}^{-1} \text{ keV}^{-1}$  and  $j^+ = 10^7 \text{ E}^{-2.5} \text{ cm}^{-2} \text{ sec}^{-1} \text{ ster}^{-1} \text{ keV}^{-1}$ . Using typical magnetopause plasma and field values of 20 cm<sup>-3</sup> and 50 nT, it is shown that the 1-10 keV electrons and protons are scattered near the limit of strong pitch angle diffusion by the observed waves. A precipitation flux of -0.15 ergs/cm<sup>2</sup> sec is calculated, indicating a significant contribution to the dayside aurora.

Introduction

It is well known that solar wind energy is transferred to the magnetosphere by processes such as magnetic reconnection (Dungey, 1961, Russell and Elphic, 1979) and viscous interaction (Eastman et al., 1976; Crooker, 1977) at the Earth's magnetopause, and is subsequently released in the night-side magnetosphere as substorms. The purpose of this letter is to demonstrate that wave-particle interactions are effective in transferring energy to the magnetosphere. Plasma instabilities at the magnetopause (Gurnett et al., 1978) can lead to rapid particle velocity space scattering and cross field diffusion. If the flux of the particles is sufficiently high and the rate of scattering is sufficiently rapid, the loss of particles to the dayside ionosphere can make a significant contribution to the dayside aurora.

The ISEE-1 and -2 wave and particle data obtained by the experiments described in Gurnett et al., (1978) and Anderson et al. (1978) have been used to perform a joint wave and particle study to determine the possible consequences of wave-particle interactions at and near the Earth's magnetopause.

Results

Plasma Waves

Figure 1, taken from Gurnett et al. (1979), illustrates the properties of the plasma waves in six crossings or near-crossings of the magnetopause, indicated by the crosshatching. For each of the events, spacecraft proximity to the magnetopause has been confirmed (D. J. Williams, personal communication) by energetic particle measurements using a technique described in Williams et al. (1980).

Intense broadband electric (10 to 10<sup>5</sup> Hz) and magnetic (10 to 10<sup>3</sup> Hz) signals are present at each magnetopause or near-magnetopause crossing. These emissions have been interpreted as a superposition of an electrostatic and an electromagnetic mode (Gurnett et al., 1979).

For a typical plasma density  $N \sim 20/\text{cm}^3$  and a magnetic field strength  $B_0 = 50 \text{ nT}$ , the electron plasma frequency and gyrofrequency are  $f_{pe} \sim 4 \times 10^4 \text{ Hz}$  and  $f_g^- \sim 1.4 \times 10^3 \text{ Hz}$ . Under the above conditions, when  $f < f_{pe}$ , the ordinary mode is evanescent. The only electromagnetic wave which can propagate is the right-hand whistler mode, which can exist for  $f \leq f_g^-$ .

Copyright 1981 by the American Geophysical Union.

Clearly defined flux transfer events have been identified at three of the six events at 1435, 1447, and 1454 UT (Russell and Elphic, 1979) by their characteristic signature in the  $B_N$  component. The other three events may also be associated with flux transfer because the variation in  $B_N$  is similar to the three previously identified events.

The peak and average spectra of the plasma wave emissions have been calculated for 10 individual magnetopause events selected at random. The magnetic spectra are shown in Figure 2 and the electric spectra in Figure 3. Both electric and magnetic spectra exhibit large intensity variations from one magnetopause event to another. Several orders of magnitude variation are shown in the figures. The spectral shapes, however, remain relatively constant. In general, the wave intensities decrease with increasing frequency, with a power law dependence. However, significant deviations from this relationship are found. For example, in the left-hand panel of Figure 3, intense emissions at  $\sim 10^4 \text{ Hz}$  indicate the presence of Langmuir waves. The turn-up of the spectra at  $f > 10^4 \text{ Hz}$  in Figure 3 is due to electromagnetic Terrestrial Kilometric Radiation (TKR).

For purposes of this paper, we have constructed an average power law spectra for both the electromagnetic and electrostatic waves. These are indicated as straight lines in the right-hand panels of Figures 2 and 3. These "typical" spectra, exclude the superposed (Langmuir and TKR) emissions and also take account of the instrument sensitivity for the low frequency electromagnetic waves. The "typical" spectral intensities are:  $I_m = 10 f^{-3.9} \text{ nT}^2/\text{Hz}$  and  $I_e = 3 \times 10^{-5} f^{2.8} \text{ V}^2/\text{m}^2 \text{ Hz}$  for the magnetic and electric components, respectively. The electric spectrum in the frequency range 10-10<sup>3</sup> Hz, is thought to be a superposition of electromagnetic and electrostatic waves. For  $f > 10^3 \text{ Hz}$ , the waves are believed to be purely electrostatic. The magnetic spectrum is due to the whistler mode waves.

From over 150 magnetopause crossings in the dawn to noon local time sector (identified by plasma and magnetic field characteristics from the ISEE data pool), magnetopause waves were detected on 85% of the crossings examined. It is possible that the emissions were present even more frequently, but their intensities were below the detector threshold. An investigation was carried out to determine if the magnetosheath magnetic field influenced the plasma wave intensity. The results indicate that wave intensities are not strongly dependent on either the magnetosheath magnetic field north-south direction or on field magnitude.

Low Energy Particles

Figure 4 illustrates the correlation typically found at the magnetopause between plasma waves, 1 - 6 keV electrons and 5.4 - 6.6 keV protons. The period when the intense broad-band plasma waves are detected is indicated by the crosshatching. The event in Figure 4 is a partial magnetopause crossing. At the left hand side of the figure, at 1400 UT, ISEE-1 is in the magnetosheath. The spacecraft crosses the magnetopause at 1441:50 UT and remains in the magnetopause until 1443:05 when the "magnetopause bulge or wave" passes over the spacecraft, again leaving it in the magnetosheath. This event is a Flux Transfer Event (Elphic and Russell, 1979).

During this traversal into the magnetopause, intense fluxes of 1.4 - 1.6 and 4.5 - 6.0 keV electrons are detected. This steplike increase in electron flux is called an "electron shoulder", a feature common to the magnetopause (Parks et al. 1979). There is a slight proton enhancement in the higher energy 5.4 - 6.6 keV channel during this event. The low energy 1.3 - 1.7 keV proton flux in the magnetopause is approximately unchanged from the magnetosheath values.

The onset and cutoff of both the waves and particles are found to be

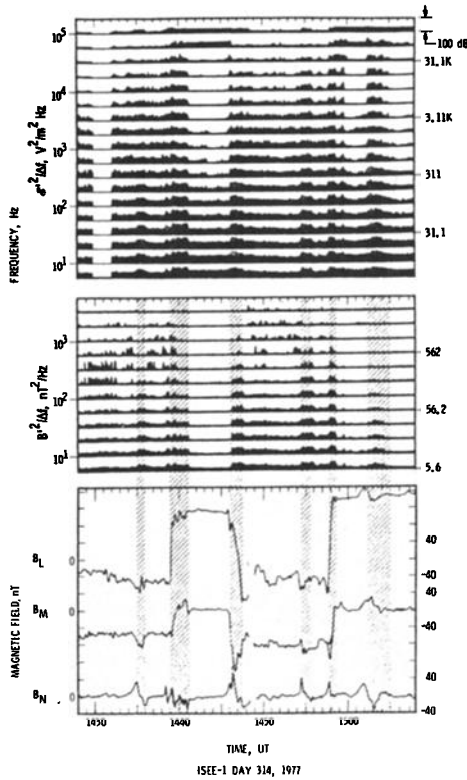


Fig. 1. Examples of the broadband plasma waves at six crossings or near crossings of the magnetopause. The plasma wave electric and magnetic spectra are illustrated in the top and middle panels, and the ambient magnetic field at the bottom. For each of the 18 electric and 13 magnetic spectral channels shown, the wave intensities are plotted logarithmically with five orders of magnitude displayed for each spectrum channel. The magnetic field is in the orthogonal NLM coordinate system, with N perpendicular to the magnetopause, L along the projection of the magnetospheric Z axis onto the magnetopause, and M completing the right hand system.

simultaneous. This correlation has been observed at many magnetopause crossings and by simultaneous ISEE-1 and -2 measurements, with suitable delays. This feature can only be explained by a very sharp outer boundary for the wave-particle layer.

Figure 5 illustrates the relationship between the plasma waves, the 1-6 keV electrons and protons and the plasma and magnetic field parameters for the six magnetopause or near-magnetopause events which were previously illustrated in Figure 1. The plasma and field data for this event have been previously examined in great detail in Paschmann et al., (1979) and Russell and Elphic (1979). For simplicity, only the electromagnetic portion of the waves is displayed, as the whistler mode and electrostatic emissions are time-coincident. Although the wave data are from

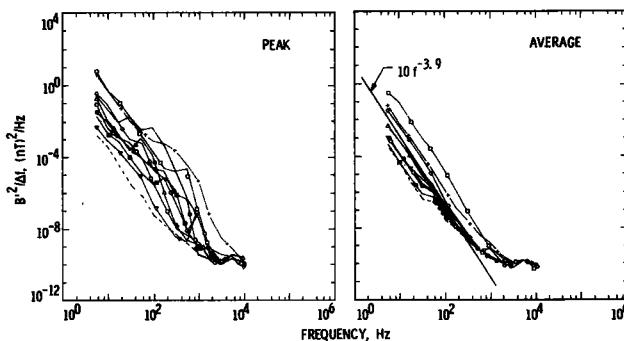


Fig. 2. The magnetic spectra for 10 randomly selected magnetopause events. The left-hand panel contains the wave peak spectra and the right-hand panel illustrates the spectral averages over the interval. A "typical" average power law wave spectrum has been added to the figure.

ISEE-1 and the particle and plasma/field plots are from ISEE-2, the time separation between the two spacecraft is only 30 seconds to 1 minute, negligible on these scales.

For each of the six magnetopause events, the relationship between the broad-band plasma waves and the 1 - 6 keV electrons and protons is similar to that in Figure 4. A correlation exists between plasma wave enhancement and the 1 - 6 keV electron and 5.4 - 6.6 keV proton flux increases for each of the six magnetopause crossings. All of the wave and particle onsets and terminations are sharp and thus easy to identify. The 1.3 - 1.7 keV magnetopause proton fluxes are essentially unchanged from magnetosheath values.

The magnetopause particle flux values are approximately constant (within an order of magnitude) during these 6 crossings and are essentially the same as those for the event in Figure 4. This relationship is found to hold true for widely varying solar wind conditions.

Because of this feature an accurate estimation of the particle spectra is possible using flux measurements at three energies (also Parks et al., 1979). From the analysis of 10 events, we obtained the following:

$$j^- = 3 \times 10^5 E(\text{keV})^{-1.8} / \text{cm}^2 \text{ sec str keV}$$

$$j^+ = 10^7 E(\text{keV})^{-2.5} / \text{cm}^2 \text{ sec str keV}$$

The multiple magnetopause crossings during this day are caused by motions of the boundary across the spacecraft. Depending on the extent of the boundary displacement, the wave-particle region is either partially crossed (1435 - 1436, 1454 - 1456 and 1501 - 1504 UT) or entirely traversed. Examples of the latter are found at 1441 and 1500 UT. Drop-outs of the 1.3 - 1.7 keV protons (and decreases of the other electron and proton fluxes) are coincident with plasma density decreases and temperature increases (third and fourth panels), indicating entry into the magnetosphere proper.

Although the correlated plasma wave and 1-6 keV particle events have been described as magnetopause events, the region is considerably wider than the nominal thickness ( $1-2 \rho_p$ ) of the magnetopause current layer. ISEE makes three traversals through the entire wave-particle layer during this period (1439 - 1441, 1446 - 1448, 1457 - 1500 UT). Of these times, the low latitude plasma boundary layer is present only once, at 1449 - 1550 UT. The extent of the wave and particle region is greater than that of the plasma boundary layer, as the former is present from 1457 to 1500. A rough estimate of the wave-particle boundary layer thickness can be made by assuming that ISEE is moving through a stationary structure. A value of 5 - 7 proton gyroradii thickness is found for these events.

The correlated plasma waves and 1 - 6 keV particles are related to Flux Transfer events for the examples shown in this note. At present it is uncertain whether this is fortuitous or is a general observation. We are presently performing a statistical analysis of numerous magnetopause crossings to determine this relationship.

#### Wave-Particle Interactions and Auroral Precipitation

Both electrons and protons can be scattered in velocity space by Doppler-shifted cyclotron resonance with fluctuating electromagnetic or electrostatic emissions satisfying the resonance condition  $\omega - k_{\parallel} |v_{\parallel}| = 2\pi n f_g^{\pm}$ . The

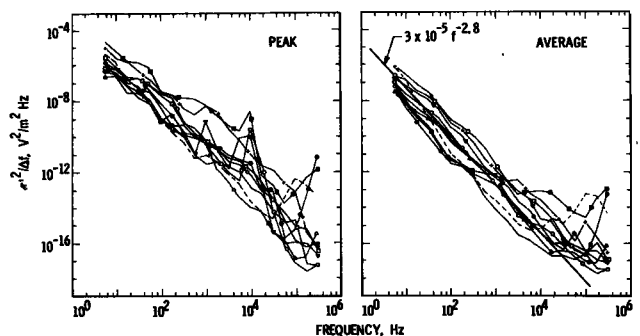


Fig. 3. Same format as Figure 2, except for the wave electric field spectra.

right-hand polarized electromagnetic emissions undergo first order ( $n = 1$ ) cyclotron resonance with electrons moving in the opposite direction to the waves. Because of the broad-band nature of the observed wave spectrum, a wide range of resonant electron energies are involved. 1 - 10 keV protons can also resonate with and be scattered by the low frequency portion of the whistler mode spectrum. Resonance with the obliquely polarized electrostatic turbulence is more complex, often involving multiple harmonic ( $n \gg 1$ ) interactions.

The effective rate of pitch-angle scattering during cyclotron resonant interaction with the fluctuating wave turbulence,  $D_{\alpha\alpha} \sim (\Delta\alpha)^2/2\Delta t$ , can be approximated by:

$$D_{\alpha\alpha}^{\pm} \sim (B'/B_0)^2 2\pi f_g^{\pm} \eta$$

$$D_{\alpha\alpha}^{\pm} \sim (c/v)^2 (\epsilon'/B_0)^2 2\pi f_g^{\pm} \eta$$

for electromagnetic or electrostatic waves with wide band amplitude  $B'$  and  $\epsilon'$  respectively. In the above expressions,  $B_0$  is the ambient magnetic field strength and  $\eta$  represents the fraction of the bounce period that the particle is in resonance with the waves. The theoretical limit of strong diffusion occurs when particles are scattered across the dimension of the atmospheric loss cone within a particle bounce time (Kennel and Petschek, 1966). For  $\eta \sim 1/5$  and field lines near the magnetopause ( $L \sim 10$ ), this requires minimum electromagnetic wave amplitudes of:

$$B'_{SD-}(m\gamma) \sim 10 E_-^{1/4} (keV)$$

$$B'_{SD+}(m\gamma) \sim 100 E_+^{1/4} (keV)$$

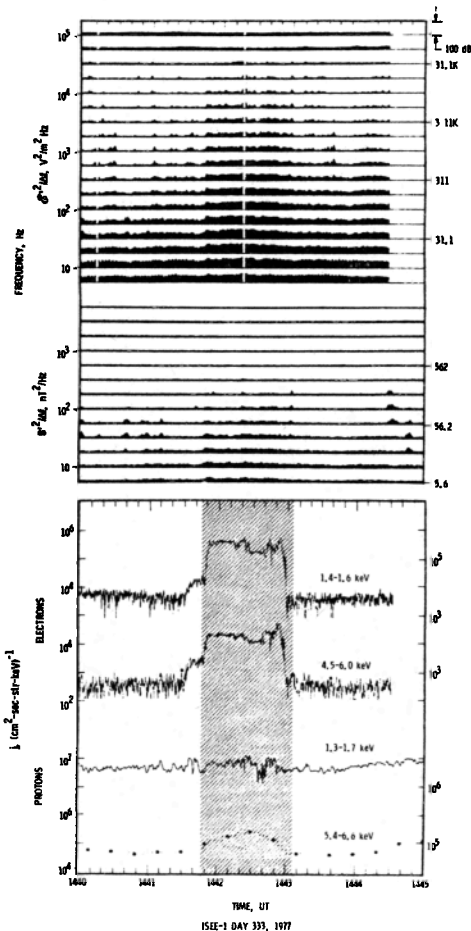


Fig. 4. An example of the strong correlation that exists between the broadband plasma waves and the 1 - 6 keV electron and the 5.4 - 6.6 keV proton flux enhancements at the magnetopause. The wave event is indicated by the cross-hatching. Areas outside the cross-hatching correspond to the magnetosheath. The 1.3 - 1.7 keV proton flux inside the wave-particle region is essentially unchanged from magnetosheath levels.

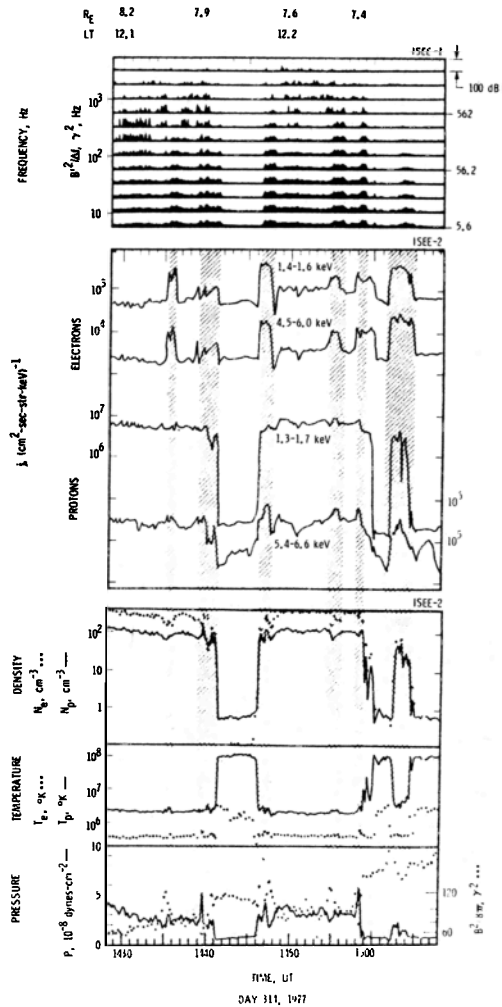


Fig. 5. The relationship between the magnetopause plasma waves (top panel), the 1 - 6 keV electrons and protons (middle) and the plasma and magnetic field parameters (bottom). The correlated plasma waves and low energy particle events are detected at each of the six crossings or partial crossings. The wave-particle region is characterized by sharp inner and outer spatial boundaries.

for ions and electrons of energy  $E_{\pm}$  (keV), respectively (Thorne and Andreoli, 1980). For strong diffusion electrostatic scattering, the required amplitudes are:

$$\epsilon'_{SD-}(mV/m) \sim E_-^{3/4} (keV)/6$$

$$\epsilon'_{SD+}(mV/m) \sim E_+^{3/4} (keV)/30$$

The mean intensity of the broad-band electromagnetic waves observed at the magnetopause are comparable to or exceed the above requirement for strong diffusion scattering of 1 - 10 keV electrons and protons. Interaction with electrostatic waves will lead to near-strong diffusion. Particles in the energy range 1 - 10 keV should thus maintain pitch angle isotropy and the precipitated energy flux into the atmosphere,  $E_{precip}$ , can be estimated as:

$$E_{precip} = 2\pi \int_{1 \text{ keV}}^{10 \text{ keV}} [j^-(E) + j^+(E)] E dE = 0.15 \text{ erg/cm}^2 \text{ sec}$$

The dayside auroral precipitation is typically  $\leq 1 \text{ erg/cm}^2 \text{ sec}$  (R. H. Eather, personal communication). The estimate calculated above indicates that wave-particle interactions at the magnetopause make a substantial contribution to this energy deposition. Protons comprise the predominant

portion of the precipitating energy flux in the range 1 to 10 keV. However, one can expect a significant flux of electrons to be present at energies below the detected range, i.e.,  $\leq 1$  keV. In agreement with this, substantial fluxes of  $\leq 500$  eV electrons are almost always found in this region of space by the LEPDEA experiments (T. E. Eastman, personal communication). These low energy electrons cannot be effectively scattered by the observed electromagnetic waves, but resonance with the electrostatic emissions could lead to strong diffusion. A joint study is currently being undertaken to determine the relationship between these  $<1.0$  keV electrons and the electrostatic emissions to determine the magnitude of additional energy contribution to the dayside aurora.

#### Relativistic Electron Precipitation

The low frequency ( $<20$  Hz) portion of the electromagnetic wave spectrum will cyclotron resonate with relativistic electrons. The wave intensities will exceed the level required for strong pitch angle diffusion. It is therefore possible the relativistic electron precipitation (REP) events which typically occur near the outer boundary of particle trapping (Brown and Stone, 1972; Thorne and Andreoli, 1980), could be caused by resonant interaction with these waves. During geomagnetically active periods, when there is sufficient inward motion of the magnetopause wave region to produce overlap with the particle outer trapping boundary, REP events would be expected. However, during more quiet periods when the region of intense waves is separate from the particle trapping region, the loss rate will be dominated by the rate of injection of relativistic electrons into the magnetopause wave-particle layer. These particles should be rapidly removed within the minimum scattering lifetime,  $\tau_L \sim 100$  sec, and will prevent the buildup of sufficient flux for REP events.

#### Conclusions

The presence of intense electromagnetic and electrostatic emissions is correlated with enhanced fluxes of 1 - 6 keV electrons and protons at the Earth's magnetopause. Wave-particle resonant interactions are sufficiently intense to lead to strong particle pitch angle diffusion, and the resultant precipitation represents a significant portion of the dayside auroral energy. The measured proton-to-electron ratio in the 1 - 10 keV energy range indicates the presence of substantial fluxes of electrons at energies outside this range, presumably below 1 keV. The interaction between these low energy electrons and electrostatic waves may account for the remaining dayside auroral precipitation energy.

Although the sources of these 1 - 10 keV magnetopause particles are not well understood at this time, the wave and particle features determined in this article give some important clues. The 1.3 - 1.7 keV proton flux was essentially unchanged as the spacecraft moved from the magnetosheath into the wave-particle layer at and inside the magnetopause. Thus, one obvious possibility is that magnetosheath protons are able to penetrate 5 - 7  $\rho_p$  across the magnetopause current layer. Cross-field diffusion by interaction with the plasma waves, is currently being investigated as a potential transport mechanism.

The 1 - 6 keV electrons and 5.4 - 6.6 keV protons have energies well above magnetosheath plasma values. Local stochastic acceleration of either magnetosheath or ionospheric plasma is one possible source for these particles. Resonant interaction with the electrostatic emissions is more effective (than with the electromagnetic emissions) in diffusing the particles in energy space because such interactions directly alter the magnitude of the particle velocity. Using the characteristic rate of energy diffusion  $D_{\perp}^{\pm} = \langle \Delta v_{\perp}^2 \rangle / 2\Delta t \sim 2\pi f_g^{\pm} c^2 (\epsilon'/B_0)^2$  (e.g., Ashour-Abdalla and Thorne, 1978) for resonant interactions with electrostatic waves, one obtains a time scale for stochastic acceleration  $\tau_E \sim (B_0/\epsilon')^2 (E_{\pm}/mc^2) / 2\pi f_g^{\pm}$ . For the average electric field intensities given in Figure 3, ion acceleration to a few keV will occur within minutes.

The consequences of the magnetopause wave-particle interactions which have been reported here are consistent with the known features of the day-

side aurora. The precipitation flux should be relatively constant and should be independent of the interplanetary magnetic field direction (and substorms). Recent optical observations (Akasofu and Kan, 1979), have demonstrated that the daytime precipitation pattern is a separate system from the nighttime precipitation, implying that two different mechanisms are in operation.

The dayside precipitation due to the magnetopause wave-particle interactions should occur at a slightly lower latitude than the contribution due to magnetosheath plasma entering the cusp. Further optical observations are needed to resolve the two regions and their properties.

#### Acknowledgements

This work was initiated and supported by the ISEE Guest Investigator program. T. Chuh and R. Okida assisted in the reduction and analysis of the data. This paper represents one aspect of research done at the Jet Propulsion Laboratory, California Institute of Technology for NASA under contract NAS 7-100. This research was also supported, in parts, by contracts NAS 5-20093 with the University of Iowa, NAS 5-25722 with the University of California at Los Angeles, NAS 5-20079 with the University of Washington and by NSF grant ATM 77 22346.

#### References

- Akasofu, S. I., and J. R. Kan, "Dayside and Nightside Auroral Arc Systems", *Geophys. Res. Lett.*, **7**, 753, 1980.
- Anderson, K. A., R. P. Lin, R. J. Paoli, G. K. Parks, C. S. Lin, H. Reme, J. M. Bosqued, F. Martel, F. Cotin and A. Cros, "An Experiment to Study Energetic Particle Fluxes in and Beyond the Earth's Outer Magnetosphere," *IEEE Trans. Geosci. Electr.*, GE-16, 213, 1978.
- Ashour-Abdalla, M. and R. M. Thorne, "Toward a Unified View of Diffuse Auroral Precipitation," *J. Geophys. Res.*, **83**, 4755, 1978.
- Brown, J. W. and E. C. Stone, "High-Energy Electron Spikes at High Latitude," *J. Geophys. Res.*, **77**, 3384, 1972.
- Crooker, N. U., "The Magnetospheric Boundary Layers: A Geometrically Explicit Model," *J. Geophys. Res.*, **82**, 3629, 1977.
- Dungey, J. W., "Interplanetary Magnetic Field and the Auroral Zones," *Phys. Rev. Letts.*, **6**, 47, 1961.
- Eastman, T. E., E. W. Hones, S. J. Bame and J. R. Asbridge, "The Magnetospheric Boundary Layer: Site of Plasma Momentum and Energy Transfer from the Magnetosheath into the Magnetosphere," *Geophys. Res. Letts.*, **3**, 685, 1976.
- Elphic, R. C. and C. T. Russell, "ISEE-1 and -2 Magnetometer Observations of the Magnetopause," *Magnetospheric Boundary Layers*, ESTEC Noordwijk, The Netherlands, 43, 1979.
- Gurnett, D. A., F. L. Scarf, R. W. Fredricks, and E. J. Smith, "The ISEE-1 and ISEE-2 Plasma Wave Investigation," *IEEE Trans. Geoscience Electron.*, GE-16, 225, 1978.
- Gurnett, D. A., R. R. Anderson, B. T. Tsurutani, E. J. Smith, G. Paschmann, G. Haerendel, S. J. Bame, and C. T. Russell, "Plasma Wave Turbulence at the Magnetopause: Observations from ISEE 1 and 2," *J. Geophys. Res.*, **84**, 7043, 1979.
- Kennel, C. F., and H. E. Petschek, "Limit on Stably Trapped Particle Fluxes," *J. Geophys. Res.*, **1**, 1966.
- Parks, G. K., C. S. Lin, K. A. Anderson, R. P. Lin, H. Reme, F. Coroniti, C. Meng, and R. Pellat, "Particle Boundary Structures at the Magnetopause and the Plasma Sheet," *Magnetospheric Boundary Layers*, ESTEC, Noordwijk, The Netherlands, 151, 1979.
- Paschmann, G., N. Scokopke, G. Haerendel, J. Papamastorakis, S. J. Bame, J. R. Asbridge, J. T. Gosling, E. W. Hones, Jr., E. R. Tech, "ISEE Plasma Observations Near the Subsolar Magnetopause," *Space Sci. Rev.*, **22**, 717, 1979.
- Russell, C. T. and R. C. Elphic, "Initial ISEE Magnetometer Results: Magnetopause Observations," *Space Sci. Rev.*, **22**, 681, 1979.
- Thorne, R. M. and L. J. Andreoli, "Mechanisms for Intense Relativistic Electron Precipitation," in *Exploration of the Polar Atmosphere*, ed. C. S. Deehr, Reidel Publ. Co., Dordrecht, Holland, in press, 1981.
- Williams, D. J., T. A. Fritz, B. Wilken, and E. Keppler, "An Energetic Particle Perspective of the Magnetopause," *J. Geophys. Res.*, **84**, 6385, 1980.

(Received October 14, 1980;  
accepted November 5, 1980.)